



PAPER

3D bioprinting of GelMA scaffolds triggers mineral deposition by primary human osteoblasts

To cite this article: Christine McBeth *et al* 2017 *Biofabrication* **9** 015009

View the [article online](#) for updates and enhancements.

You may also like

- [Fabrication of poly\(ethylene glycol\): gelatin methacrylate composite nanostructures with tunable stiffness and degradation for vascular tissue engineering](#)
Peter Kim, Alex Yuan, Ki-Hwan Nam et al.
- [Electrospun gelatin-based scaffolds as a novel 3D platform to study the function of contractile smooth muscle cells *in vitro*](#)
J C Bridge, M Amer, G E Morris et al.
- [Effect of sterilization treatment on mechanical properties, biodegradation, bioactivity and printability of GelMA hydrogels](#)
Muhammad Rizwan, Sarah W Chan, Patricia A Comeau et al.

Biofabrication



PAPER

3D bioprinting of GelMA scaffolds triggers mineral deposition by primary human osteoblasts

Christine McBeth¹, Jasmin Lauer¹, Michael Ottersbach², Jennifer Campbell¹, Andre Sharon^{1,3} and Alexis F Sauer-Budge^{1,4,5}

¹ Center for Manufacturing Innovation, Fraunhofer USA, Brookline, MA 02446, USA

² Fraunhofer Institute for Production Technology, Aachen, Germany

³ Department of Mechanical Engineering, Boston University, Boston, MA 02215, USA

⁴ Department of Biomedical Engineering, Boston University, Boston, MA 02215, USA

⁵ Author to whom any correspondence should be addressed.

E-mail: asauerbudge@fraunhofer.org

Keywords: bioprinting, GelMA, gelatin methacryloyl, scaffold, mineral deposition, osteoblast

Supplementary material for this article is available [online](#)

RECEIVED
16 September 2016

REVISED
29 November 2016

ACCEPTED FOR PUBLICATION
14 December 2016

PUBLISHED
10 January 2017

Abstract

Due to its relatively low level of antigenicity and high durability, titanium has successfully been used as the major material for biological implants. However, because the typical interface between titanium and tissue precludes adequate transmission of load into the surrounding bone, over time, load-bearing implants tend to loosen and revision surgeries are required. Osseointegration of titanium implants requires presentation of both biological and mechanical cues that promote attachment of and trigger mineral deposition by osteoblasts. While many factors contribute to differentiation, the relative importance of the various cues is unclear. To substantially improve osseointegration of titanium implants, we generated a gelatin methacryloyl (GelMA) scaffold, using an extrusion-based 3D bioprinter, which can be directly printed on and grafted to the titanium implant surface. We demonstrate that this scaffold is able to trigger mineral deposition of both MG63 osteoblasts and primary normal human osteoblasts in the absence of any exogenous osteogenic factors. Films of the same formulation failed to promote mineral deposition suggesting that the three dimensional scaffold was able to tip the balance in favor of differentiation despite other potentially unfavorable differentiation cues of the material. We further show that these GelMA lattices can be directly grafted to titanium alloy and are secure *in vitro* over a period of seven weeks. When grafted within a groove system, the GelMA hydrogel is protected from shearing forces in a marrow implantation model. This prepares the way for osteogenic coatings to be directly manufactured on the implant surface and packaged for surgery.

Introduction

Successful osseointegration of titanium-based implants for total hip arthroplasty (THA) involves a complex series of biological processes, beginning with attachment of bone-producing osteoblasts [1]. At the implant surface, migrating pre-osteoblasts can attach and differentiate into mature osteoblasts that deposit mineral when appropriate biological and physical cues are present [2]. These maturing cells substantially contribute to the generation of new, native bone that has the mechanical strength to endure the repeated loading of normal movement. The decision to

continue proliferation or switch to a differentiation pathway is a critical one [3]. When pre-osteoblasts fail to differentiate at the implant surface, they proliferate into fibrous sheets that lack the mechanical strength required to transmit the load across the bone-implant joint, often leading to implant failure [4].

The signals that pre-osteoblasts require to make decisions about differentiation can be largely divided into molecular and mechanical. On the molecular side, several factors have been identified including inorganic calcium-phosphate crystals that make up 70% of native bone and arginine-glycine-aspartate (RGD) motifs of the collagen protein fibrils that

comprise the remaining 30% [5–7]. Growth factors such as bone morphogenetic protein 2 (BMP2) also play a role in promoting bone growth and have been incorporated into several osteoinductive scaffolds [8, 9]. *In vitro*, osteogenic media containing glucocorticoids and β -glycerophosphate are often used to boost the expression of differentiation responses to a variety of surfaces via upregulation of specific transcription factors [10, 11]. On the mechanical side, numerous studies have made it clear that smooth titanium surfaces ($R_a \approx 0.2$) promote fibrous tissue while rough titanium surfaces ($R_a \approx 2.0$) are more often surrounded with new bone growth [12, 13]. Material elasticity also plays a role for differentiating osteoblasts with hard materials such as glass, tissue culture treated plastic, and titanium promoting mineral deposition to a greater degree than synthetic polymers and hydrogels [14]. In addition to roughness and elasticity, significant differentiation has been shown to occur due to porous environments with pore sizes in the 200–550 μm range and mathematical modeling suggests that optimal ingrowth can extend up to 800 μm [15, 16]. Porous environments allow for vascularization, facilitating the generation of healthy tissue. Thus, special coatings for titanium implants that improve osseointegration should incorporate both the molecular and mechanical features that cue migrating pre-osteoblast populations to attach and mature, and allow for healthy tissue formation. However, the hierarchy of these cues is largely unclear.

Designing and fabricating scaffolds that incorporate both biological and physical cues that trigger osteodifferentiation is an active area of research collectively known as bone tissue engineering [17]. These scaffolds vary greatly in terms of material choice (polycaprolactone, glycidyl methacrylated dextran, titanium, etc) and manufacturing methods (selective laser sintering, direct casting, etc) [18, 19]. Gelatin methacryloyl (GelMA) is a modified gelatin hydrogel that is emerging as a superior tissue engineering base material due to its natural RGD and matrix metalloproteinase (MMP) moieties that promote biological interaction, low antigenicity, high versatility in terms of manufacturing methods, tunability for controlling material properties, stability at physiological temperatures, and low cost [20, 21]. Research using GelMA hydrogels for promoting the osseointegration of titanium implants has been focused on chemically grafting GelMA to the implant surface, and longitudinal studies with osteoblasts have been limited [22].

For our work here, we monitored cytoskeletal organization and new mineral deposition in response to a subset of biological and mechanical cues in the absence of exogenous osteogenic media. We demonstrate that the biological cues provided by the GelMA hydrogel were unable to overcome the countercue of a soft surface in terms of appropriately organizing the cytoskeleton. To mimic the critical spatial cues of rough pores in the 200–500 μm range that support

differentiation, it was necessary to be able to build the hydrogel construct into a three-dimensional porous structure. For this purpose, we used our in-house multi-material rapid prototyper for 3D bioprinting [23]. We were able to generate hydrogel lattices with pore sizes $\sim 400 \times 400 \mu\text{m}$. We show that the printed lattice structure alone is sufficient to trigger mineral deposition in the absence of any exogenous biological factors in both the osteoblast cell line MG63 and primary normal human osteoblasts (NHObst). To demonstrate the feasibility of incorporating this lattice into a manufacturing workflow, we directly bioprinted and grafted these structures to titanium alloy substrates and tested the durability of GelMA-coated titanium in a marrow implantation model. These results support the use of GelMA as an excellent candidate for improving the osseointegration of titanium implants.

Materials and methods

Culture of MG63 and NHObst cells

MG63 osteoblast-like cells (ATCC) were cultured and maintained in Eagle's minimum essential medium (EMEM, ATCC) supplemented with 10% heat-inactivated fetal bovine serum (FBS) and 100 U ml^{-1} penicillin and 100 U ml^{-1} streptomycin (Thermo Fisher Scientific). MG63 cells were passaged every 3–4 d, as required. Primary normal human osteoblasts (NHObst) were cultivated in osteoblast basal medium (OBM) supplemented with SingleQuots of ascorbic acid, gentamicin, and FBS (Lonza) according to manufacturers' protocols. NHObst were plated for experiments when between 4–6 doublings.

Gelatin methacryloyl (GelMA) hydrogel

GelMA was synthesized in-house with type B porcine skin gelatin (Sigma-Aldrich) by dissolving gelatin at 10% (w/v) in PBS in a water bath set to 60 $^{\circ}\text{C}$ and stirring until fully dissolved, as previously described [22]. Methacrylic anhydride (Sigma-Aldrich) was added to the gelatin solution at 50 $^{\circ}\text{C}$ at a rate of 0.5 ml min^{-1} to generate a 20% (v/v) solution of GelMA within a chemical fume hood. After a one-hour reaction time, the solution was diluted five-fold with the addition of warm (40 $^{\circ}\text{C}$) PBS and dialyzed against ddH₂O for seven days (SnakeSkin, 10 000 MWCO, Pierce). Dialyzed GelMA was snap frozen with liquid nitrogen, lyophilized (Labconco), and stored at -20°C with desiccant until further use. Buffer waste was disposed of as hazardous waste due to the presence of unreacted methacrylic acid. GelMA was rehydrated at 8% (w/v) with 0.5% (w/v) Irgacure-2959 (2-Hydroxy-4'-(2-hydroxyethoxy)-2-methylpropiophenone) as a photoinitiator in PBS warmed to 80 $^{\circ}\text{C}$. To determine the viscoelastic properties of the synthesized GelMA and to ensure batch-to-batch consistency of our methods, the shear complex modulus G^* of GelMA was measured by solid state

rheometry (AR2000 Rheometer, TA Instruments). Prior to measurement, GelMA substrates were cured with UV, peak $\lambda = 365$ nm, at an intensity of 6.9 mW cm^{-2} for 900 s. The oscillatory shear deformation was monitored using a 40 mm diameter parallel plate geometry at a constant shear strain of 2.43 mrad and frequency of 1 Hz with temperature scan ranging from 20–45 °C in 0.8 °C increments.

***In vitro* degradation of GelMA hydrogels**

GelMA (8% (w/v)) hydrogel plugs were generated in the bottom of microcentrifuge tubes and were UV cured at an intensity of 6.9 mW cm^{-2} for 5, 30, 60, or 900 s as indicated. Hydrogel plugs were incubated in the presence of collagenase II (2 U ml^{-1} ; Thermo Fisher Scientific) at 37 °C as previously described [24]. Wet weights were measured at the time points shown after a brief wicking to remove excess solution.

Bioprinting GelMA lattices for osseointegration

Our in-house designed and built bioprinter [23] was programmed to deliver GelMA material onto either poly-D-lysine treated glass coverslips or functionalized titanium sheets in a modified log cabin lattice. Three layers were printed giving a total thickness of approximately $750 \mu\text{m}$ and using approximately 150–200 μl GelMA material. Unfunctionalized gelatin layers were printed within the lattice as a support material with layer 2 offset from layers 1 and 3 by one material thickness. Lattices were UV cured for 900 s (6.9 mW cm^{-2}). Bioprinted lattices were then incubated with PBS at 37 °C to remove the gelatin support material before being seeded with 5×10^4 cells (MG63 or NHOst). Media was changed every 3–4 d and cells were cultured for 21 d before staining with Alizarin Red S (ARS) or OsteoImage as described. GelMA (200 μl) was spread on poly-D-lysine treated glass coverslips in a thin film, UV cured as before, and plated with either MG63 or NHOst cells as a control. The films had a similar thickness to the average lattice thickness (413 μm and 500 μm , respectively).

ARS, OsteoImage, and actin staining

To test attachment and mineral deposition, glass coverslips (12 mm round, VWR) were coated with poly-D-lysine (Sigma-Aldrich) to facilitate GelMA adhesion to glass. GelMA was either formulated with no BMP-2, 10 ng ml^{-1} BMP-2 ('BMP-2 lo'), or 100 ng ml^{-1} BMP-2 ('BMP2-hi'). An aliquot of the GelMA formulation at pH 7 (15 μl) was introduced in a thin film onto each coverslip and was treated with UV as before. MG63 cells (5×10^4) were seeded onto the coverslips or directly onto the plastic well as indicated. Cells were allowed to adhere for 24 h at 37 °C. After incubation, cells were washed with PBS and then fixed with 4% paraformaldehyde (PFA) in PBS for 10 min at 37 °C and washed three more times in PBS. Autofluorescence was quenched by a similar

incubation in 50 mM NH_4Cl (Sigma-Aldrich). The coverslips were then treated with blocking buffer (2% bovine serum albumin (BSA) and 2% goat serum in 50 mM NH_4Cl) for 20 min at 37 °C. Cells were then permeabilized with 0.05% saponin in PBS at room temperature for 10 min. Saponin (0.05%) was included in all subsequent wash and staining steps because using methanol as a permeant destroys the hydrogel matrix. Actin filaments in the cells were stained with FITC-phalloidin ($50 \mu\text{g ml}^{-1}$, Sigma-Aldrich) for 1 h. Calcium deposits were stained with either ARS (EMD Biosciences) or OsteoImage (Lonza) according to manufacturers' protocols. For fluorescent labeled cells, samples were mounted onto glass slides (VWR) using a mounting media (ProLong Gold, Thermo Fisher Scientific). Slides were cured for 24 h and visualized by confocal microscopy (Olympus FV1000 scanning confocal microscope with 405 nm and 454 nm excitation lines). The degree of actin filament formation was determined as previously described [25]. Briefly, images were scored in two independent blind trials on a scale from 1–5 with cells scoring 1 primarily containing cortical actin and cells scoring 5 primarily containing thick actin filaments that stretched across the entire cell. More than 20 cells were scored for each condition.

Testing osteoblast migration with GelMA hydrogels

Transwell® polycarbonate membrane inserts (Sigma-Aldrich) were used to assess MG63 migration in the presence or absence of GelMA with or without BMP2 (Life Technologies). An aliquot of 8% GelMA at pH 7 (100 μl) was dispensed in the bottom of a 24-well plate where indicated and treated with 60 s UV. BMP2 (100 ng) was either mixed with GelMA before UV treatment or into 600 μl media as indicated. Growth media (600 μl) was added to the bottom of each compartment and 100 μl of cells at 1.5×10^5 MG63 cells ml^{-1} were added to the top of the insert. Cells were allowed to migrate at 37 °C with 5% CO_2 for 24 h. The top of the inserts were then washed 2× with 200 μl PBS and wiped once with a cotton swab. Membranes were then fixed in 4% PFA (Fisher Scientific) in PBS for 10 min followed by a five minute incubation in nucleic acid stain 2-(4-Amidinophenyl)-6-indolecarbamide dihydrochloride (DAPI, Sigma-Aldrich). Migration was determined by counting nuclei under a fluorescent microscope in eight separate fields of the membrane at 20×. These results were verified by imaging the entire membrane at 4× and automatically counting nuclei by finding local maxima using ImageJ (NIH). The experiment was independently repeated three times and displayed results are representative of trials.

Titanium surfaces and implants

Parameter tests were conducted on forged and untreated TiAl_6V_4 blocks to evaluate the machinability

of differentially treated titanium parts. During milling, the titanium workpieces showed no significant differences in terms of machinability, cutting forces, or lifetime of the tools. Therefore, untreated titanium blocks were used to evaluate adhesion of bioprinted lattice scaffolds on different surface structures. TiAl_6V_4 samples with dimensions of $12 \times 12 \times 36$ mm were manufactured. The surfaces were generated by milling on a 5-axis milling machine center Heller MCi25. The aim was to generate different structures and roughness values by varying the process parameters of cutting width a_e (0.6 mm; 1.0 mm; 1.25 mm; 1.5 mm) with constant feed per tooth f_t (0.1 mm), cutting velocity v_c (120 m min^{-1}) and cutting depth a_p (0.6 mm). Twelve samples were generated for each set of parameters. The theoretical roughness values perpendicular to feed direction are in the range from $R_{\text{th}} = 9.01 \mu\text{m}$ to $R_{\text{th}} = 56.57 \mu\text{m}$.

Preparing titanium surfaces by chemical modification

Titanium was prepared for grafting as previously described [22]. Briefly, $\frac{1}{2}$ " circles or squares cut from 0.127 mm thick titanium shim (grade 2, McMaster Carr) were ultrasonically cleaned in successive baths of ethanol, acetone, and distilled water. Cleaned Ti squares were activated by soaking in 5 M NaOH (Sigma-Aldrich) at 80°C for 24 h in a reflux apparatus within a chemical fume hood. Oxidized titanium samples from this step (Ti-OH) were then functionalized by soaking in 3-(trimethoxysilyl) propyl methacrylate (TMSPMA) (10% v/v in toluene, Sigma-Aldrich) at 100°C for 24 h. Ti-TMSPMA squares were then rinsed with alcohol and acetone and allowed to air dry. Contact angle goniometry measurements were conducted by adding $2 \mu\text{l}$ ddH₂O to the prepared surface and measuring the angle (θ) between the drop and the surface on a Kruss DSA100 contact angle goniometer. θ values equal to zero indicate perfect wetting while θ values equal to 180° are perfectly non-wetting. Values are displayed as the mean measurement of five distinct sections of each surface indicated with error bars (1 standard deviation) and are representative of two independent trials. Fourier transform infrared spectrometry (FTIR) was performed on a Bruker Vertex70v FTIR with Hyperion Microscope at a resolution of 0.16 cm^{-1} . Each surface was measured in five distinct sections. GelMA was grafted to the Ti-TMSPMA squares by heating the GelMA to 37°C and directly applying the GelMA to the square by spreading the GelMA across the square. The Ti-TMSPMA was pre-heated to 37°C to facilitate even GelMA application. The final step of the grafting procedure was to treat the Ti-GelMA squares with UV light for 900 s (6.9 mW cm^{-2}). Ti-GelMA squares were subsequently rinsed in ddH₂O for 2 h to remove excess un-grafted GelMA that would interfere with downstream analyses. Titanium alloy milled squares and titanium alloy

implants fabricated from $\text{Ti}_6\text{Al}_4\text{V}$ (Fraunhofer IPT and CMI) were prepared with a TMSPMA surface coating as described above. GelMA lattices were printed onto the surfaces and were UV treated as before.

Marrow implantation models

Porcine ribs and bovine femurs were purchased from a local butcher. The porcine rib bone was broached and reamed with custom piezoelectric tools to precisely match the dimensions of the implant and to approximate the process of THA clinical procedures. Implants were inserted into the marrow and removed immediately for evaluation of grafting durability during implantation. Bovine femur marrow was broached and reamed with a drill bit matching the dimensions of the grooved rod implant and GelMA-coated implants were implanted and removed as before.

Results

GelMA hydrogels tuned for bioprinting and cellular interaction

Osteoblasts are exquisitely sensitive to both the biological and mechanical cues in their environment [2, 12]. Incorporating these cues into titanium implants and improving osseointegration is an active area of research. This is particularly true given the rising number of revision surgeries required due to an increasing number of young patients undergoing THA surgeries and the aging population [26]. In preparing a special coating for titanium implants that would promote osseointegration, we hypothesized that a porous three-dimensional lattice would be critical to differentiation when compared to smooth hydrogel films. Previous research in the osteomimetic field indicates that osteoblast precursor cells in porous environments ($150\text{--}600 \mu\text{m}$ pores, 20%–50% porosity) differentiate into osteoconductive phenotypes [27]. In selecting the base hydrogel for our osteoconductive coating, we sought a material with which we could appropriately balance both the biological demands of the cells and the mechanical demands of the bioprinter as these two requirements are often at odds. With respect to biology, the hydrogel needs to be non-toxic to cells and incorporate RGD motifs to allow for integrin-based cellular adhesion. It should additionally be stable at physiological temperatures and be able to eventually biodegrade *in vivo* and be replaced by new bone growth. On the mechanical side, in order to be bioprinted on our instrument, the hydrogel storage modulus G' value needs to be between $10^2\text{--}10^3 \text{ Pa}$ or the material is either too fluid or too stiff to print effectively. Additionally, the hydrogel needs to be secured to the titanium implant through chemical grafting to withstand the mechanical forces of implantation.

Gelatin methacryloyl (GelMA) effectively answered many of the demands of our desired bioink [20, 28]. GelMA has received much attention recently in the field of tissue engineering due to its biocompatibility and its excellent tunability. GelMA is derived from gelatin, a degraded form of collagen—the main organic component of bone—and contains RGD motifs that allow for integrin-based cellular adhesion. Adhesion is mediated by RGD-integrin interactions and is the critical first step to robust intracellular signaling and downstream differentiation as other cues are integrated [29]. Additionally, this hydrogel can be processed by cellular enzymes (collagenases) and thus potentially replaced by new bone growth [24]. GelMA is modified with methacrylate groups that allow for UV cross-linking to significantly increase material stability at physiological temperatures. Thus, while gelatin becomes a liquid at temperatures above 35–37 °C, UV cross-linked GelMA maintains its structure. Therefore, we could bioprint GelMA in a softer state ($G' = 100$ Pa) suitable for the instrument and then UV-cure it post-printing ($G' = 1000$ Pa) to ensure stability and appropriate biomechanical elasticity. Additionally, the methacrylate groups allow for grafting to the titanium implant surface [22].

To match the demands of our bioprinter and to be suitable as a chemically grafted special coating for titanium implants, we fabricated a GelMA hydrogel as described previously [24] and reconstituted it at 8% (w/v). Our goal was a final material (post-UV treatment) with a storage modulus on the order of 1 kPa, which was achieved and used for all experiments. This value is on the low end of commonly used GelMA hydrogels but was selected to promote osteoblast ingrowth, degradation, and ultimate tissue replacement of the scaffold over a period of 3–4 weeks. After synthesis, we verified that our material was non-toxic (supplemental figure 1(A)). Additionally, we tested the effects of UV treatment on the degradation kinetics of GelMA *in vitro* by incubating different GelMA samples with collagenase II (supplementary figure 1(B)). We found that our GelMA hydrogels with short UV exposures lost around 80% of their mass at Day 1 and 100% of their mass by Day 4. GelMA samples with longer UV cure times maintained around 50% of their mass through Day 4 and still had 20% of their mass at Day 18. While collagenase II enzymatic degradation assays cannot accurately recapitulate the complex degradation dynamics *in vivo*, the assay did allow us to select a UV cure time (900 s) that would likely yield a GelMA hydrogel with sufficient structure after 3–4 weeks in cell culture.

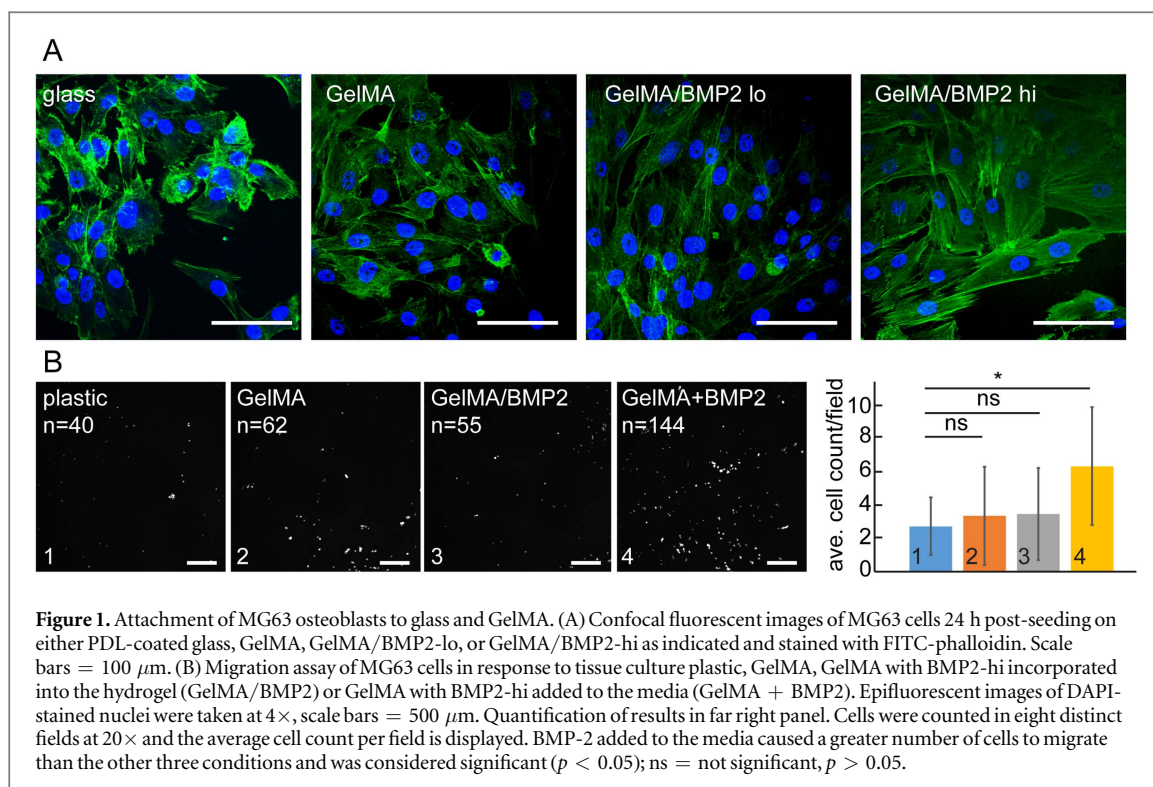
GelMA films reorganize cytoskeleton towards non-differentiating actin filament phenotype

Elasticity of the underlying substrate in osseointegration applications has been shown to play a significant role on cellular behavior [30]. For osteoblasts, harder

support materials are correlated to increased levels of differentiation [14]. Because the material elasticity of hydrogels can be relatively low when compared to collagenous bone or titanium, differentiation may be hindered on these surfaces without compensatory design. Actin filaments play a significant role in responding to mechanical cues and cytoskeletal organization can be an early indicator of ultimate cellular response [31].

In studying osteoblast responses to engineered surfaces, we and others have turned to MG63 cells. MG63 cells are an osteoblast-like cell line that are able to differentiate into mature osteoblasts and are used as a model system for studying the early mechanics of differentiation [32]. MG63 cells mimic natural osteoblast attachment better than other cell lines as they express similar integrin profiles [33]. They also most closely match natural osteoblast osteocalcin production when grown in differentiation media [34]. MG63 actin filaments form substantially longer stress fibers when grown on soft gelatin versus stiff collagen and these long actin stress fibers are correlated with lower levels of osteoblast differentiation [31, 35, 36]. Additionally, MG63 actin filaments are 4× shorter on rough titanium surfaces than smooth titanium substrates and long filaments were likewise correlated with less differentiation [36]. This trend holds true for primary normal human osteoblasts as well, indicating that early actin morphology (24 h post-plating) may portend later differentiation decisions [31].

We monitored actin filament formation in MG63 cells grown on GelMA films as an early morphological indicator of differentiation potential. Long, discrete actin filaments that extended through the cell were readily detected in cells grown on GelMA films but not glass (figure 1(A); with calculated actin scores as described in the methods section: actin score_{glass} = 1.95 ± 0.69 ; actin score_{GelMA} = 3.14 ± 0.98 , $p = 1.0 \times 10^{-5}$). This suggested that these soft GelMA films ($G' = 1$ kPa) would be a poor substrate for differentiation without compensatory design. Addition of osteoblast growth factor bone morphogenetic protein 2 (BMP2) to the GelMA films did not affect cytoskeletal organization; these samples also showed long actin filaments (figure 1(A); GelMA/BMP2 lo & hi). We investigated BMP2 release by measuring the ability of BMP2-laced GelMA films to cause MG63 migration in a standard two-well assay (figure 1(B)). MG63 cells in the top compartment were exposed to media with either GelMA or GelMA/BMP2 films on the well floor of the bottom compartment. MG63 cell migration was not significantly different when exposed to GelMA/BMP2 when compared to GelMA film and tissue culture treated plastic controls. Migration only significantly increased when BMP2 was added directed to the media (GelMA + BMP2) to mimic 100% release. Therefore, BMP2 was likely trapped within the hydrogel matrix at this early time point. While GelMA can



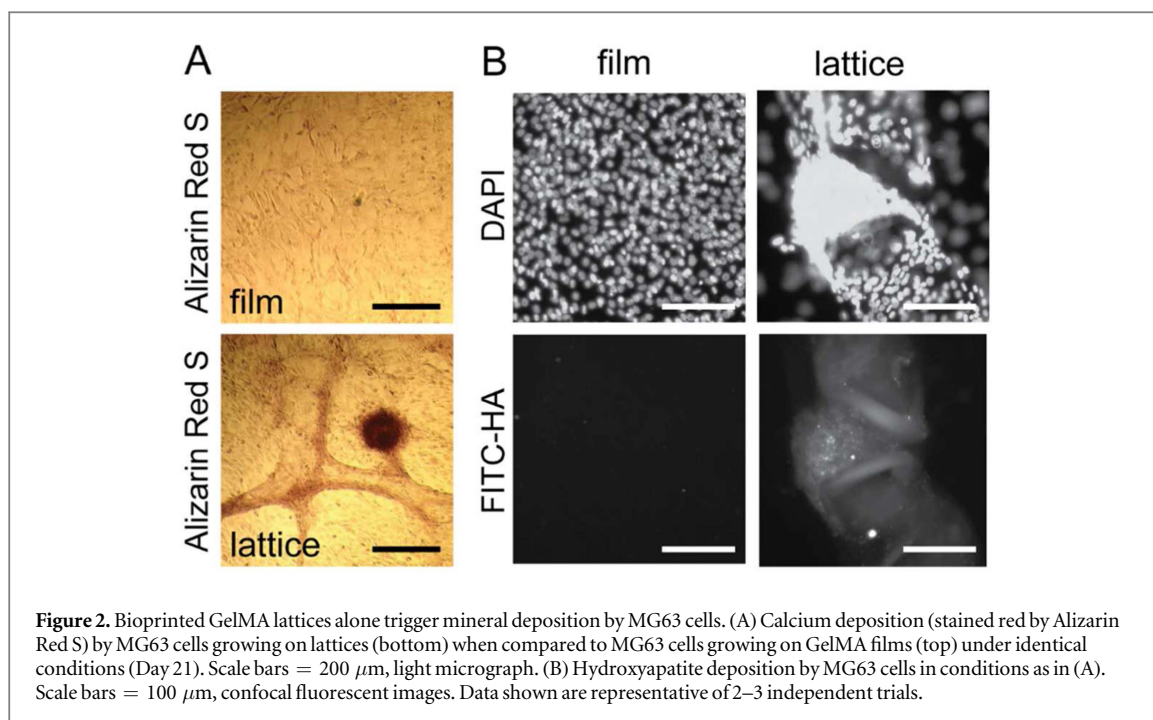
be tuned to a much higher material elasticity through increasing the level of crosslinking [28], we maintained a low stiffness regime to facilitate eventual replacement of the GelMA scaffold with cellular material and new bone growth. Together, these data suggest that the biological cues provided by the GelMA could not overcome the negative effects of a mechanically soft surface in terms of appropriately reorganizing the cytoskeleton (away from actin filaments).

Bioprinted GelMA lattices alone trigger mineral deposition by MG63 cells

We sought to compensate for the soft hydrogel by providing the spatial cues that can promote effective differentiation, and designed a lattice that could be bioprinted using our in-house 3D bioprinter. Our bioprinter is capable of delivering multiple materials to the implant surface, which allows us to build stable lattices with sacrificial materials in the negative space [23]. Pore sizes were $\sim 400 \mu\text{m} \times 400 \mu\text{m}$, approximately the dimensions previously shown to induce differentiation of osteoblasts [37]. Using an 8% GelMA solution and a 5% gelatin support material that would quickly dissolve at temperature, we printed lattices on glass coverslips to test cellular responses. UV treatment post-printing ensured that the GelMA lattice would remain stable at 37 $^{\circ}\text{C}$. GelMA lattices have been used in recent years as tissue engineering scaffolds in other applications but not with respect to bone [38–41].

To test whether the bioprinted lattice would trigger differentiation and deposition of new calcium phosphate mineral in the absence of exogenous

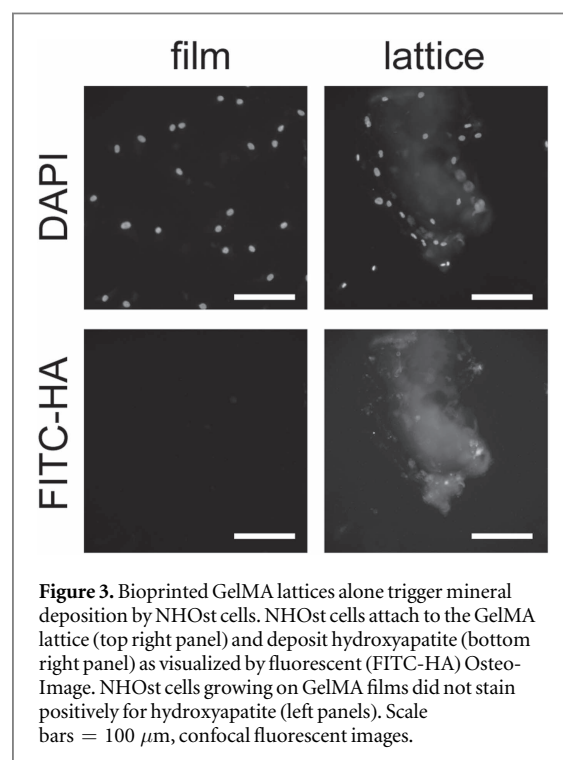
osteodifferentiation media, we incubated MG63 cells on either GelMA films or GelMA bioprinted lattices for three weeks. Both lattice and films were generated on flat substrates. After the three-week incubation period, we stained for new calcium mineral deposition by either ARS or OsteoImage. ARS binds specifically to calcium mineral while OsteoImage binds to the calcium phosphate crystal hydroxyapatite and is FITC-tagged (FITC-HA). Both are used to monitor calcium deposition of osteoblasts as only differentiating, not merely proliferating, osteoblasts produce fresh mineral, making mineral deposition the best direct indicator of differentiation [11]. During the three-week course of the experiment, media was changed every 4–5 d and additives that trigger or support differentiation were not used at any time. As suggested by the initial actin staining, MG63 cells grown on GelMA films did not deposit new mineral (figure 2). When comparing GelMA films to GelMA lattices, we found that MG63 cells deposited new calcium phosphate mineral only in the presence of GelMA lattices (figure 2(A)). Indeed, after the three-week period, MG63 cells can be seen to invade the GelMA lattice itself, grow within the hydrogel, and deposit mineral (figure 2(B)). This suggested that the spatial cues of the lattice itself trigger differentiation and that the counter-cue of material softness could be overcome by providing a porous structured environment. Therefore, in terms of future manufacturing, simple dip coatings of GelMA alone on the titanium implants would be less likely to support osseointegration.



Bioprinted GelMA lattices alone trigger mineral deposition by primary normal human osteoblasts

Having demonstrated that bioprinted GelMA lattices alone were able to induce differentiation of MG63 cells in the absence of any supporting differentiation media or biological factors, we next determined whether bioprinted lattices could trigger differentiation of primary normal human osteoblasts (NHOst). An important caveat of any study using cell lines derived from a cancer (e.g., MG63 cells) is that any observed phenotype may be unique to that cell line and may or may not be representative of what occurs in natural healthy cells [33]. Therefore, it is essential to test primary cell lines obtained directly from healthy patients.

We tested NHOst cells in the presence of either GelMA films or GelMA lattices for three weeks. Media was changed every 3–5 d as before. Media for NHOst included ascorbic acid according to the suppliers' protocols for standard support media for primary cells that are often difficult to grow but did not contain further additives that trigger or support differentiation (e.g., hydrocortisone-21-hemisuccinate, β -glycerophosphate) at any time. As shown in figure 3, NHOst cells adhered to the GelMA lattice and also grew within the hydrogel. NHOst lattices also stained positive for hydroxyapatite mineral indicating that GelMA lattices trigger differentiation of NHOst cells even without differentiation media. No such staining was seen when cells were grown on smooth films under identical conditions. This supports the finding that osteoblasts, in addition to biological cues such as BMP2 and RGD motifs, rely on mechanical and spatial cues for differentiation. Specifically, GelMA-based hydrogels in three-dimensional conformations that incorporate



porous features are particularly well-suited to providing an osteogenic environment.

Grafted GelMA bioprinted lattices adhere to titanium

In order to promote long-term osseointegration, hydrogel scaffolds and other osteoconductive coatings must be physically secured to the implant surface. Many approaches have been investigated including layer-by-layer growth [42] and photochemical grafting [43]. For the application here, the vinyl moiety of the

GelMA methacrylate groups provides an active chemical group that could be chemically bonded to functionalized titanium [22]. This procedure involves modifying the titanium surface by first treating the implant with sodium hydroxide and then 3-(Trimethoxysilyl)propyl methacrylate (TMSPMA). Previous studies demonstrated that GelMA films grafted by this method are stable on pure titanium for 3 days in simulated body fluid [22]. Furthermore, there was no delamination despite multiple wash steps and a freeze-drying process. However, whether this method would be sufficient for securing GelMA lattice scaffolds that contact the implant surface at approximately 50% less surface area than films over long periods (7 weeks) *in vitro* was unknown. Additionally, titanium implants used in THA surgeries are typically fabricated from TiAl₆V₄ which demonstrates lower rates of corrosion *in vivo* than pure titanium [44]. Whether or not titanium alloys are suitable substrates for GelMA grafting was also uncertain.

To address these issues, we bioprinted GelMA lattice scaffolds onto TiAl₆V₄ and monitored attachment *in vitro* over the course of seven weeks at 37 °C. We tested TiAl₆V₄ implants of varying calculated surface roughness to determine the role that surface roughness has in adherence of GelMA lattice scaffolds. The machined surfaces had 0.6 mm, 1.0 mm, 1.25 mm, and 1.5 mm spaced surface features which corresponded to R_{th} values of 9.01 μm , 25.06 μm , 39.21 μm , and 56.57 μm , respectively (figure 4(A)). Each of these surface roughness values were selected to provide mechanical cues that promote differentiation of osteoblasts for cells contacting the implant in the pores of the lattice [12]. Bioprinted GelMA lattices on the TiAl₆V₄ surfaces are shown in figure 4(B). GelMA lattices were bioprinted onto either untreated titanium (Ti), titanium treated with sodium hydroxide (Ti-OH), or titanium fully functionalized with TMSPMA (Ti-T) (figure 4(C)). Samples were then UV treated to stabilize the GelMA and to chemically cross-link the GelMA to the titanium surfaces. Attachment of the GelMA lattices to the titanium surfaces was scored at the time points indicated by percentage of total hydrogel affixed to the surface. All of the bioprinted GelMA lattices on untreated TiAl₆V₄ surfaces detached within the first 24 h. Treatment with sodium hydroxide (Ti-OH) substantially improved the longevity of the bioprinted lattices with 40%–60% of the lattice still attached on all four surface roughnesses after 1 month. Full functionalization with TMSPMA yielded 80% attachment for at least 7 weeks for the two surfaces with the lowest degree of surface roughness.

Grafted GelMA protected by grooved implants in bovine femur implantation model

Implantation of titanium prostheses during THA surgery requires considerable force to drive the implant into the femoral shaft. During THA, the

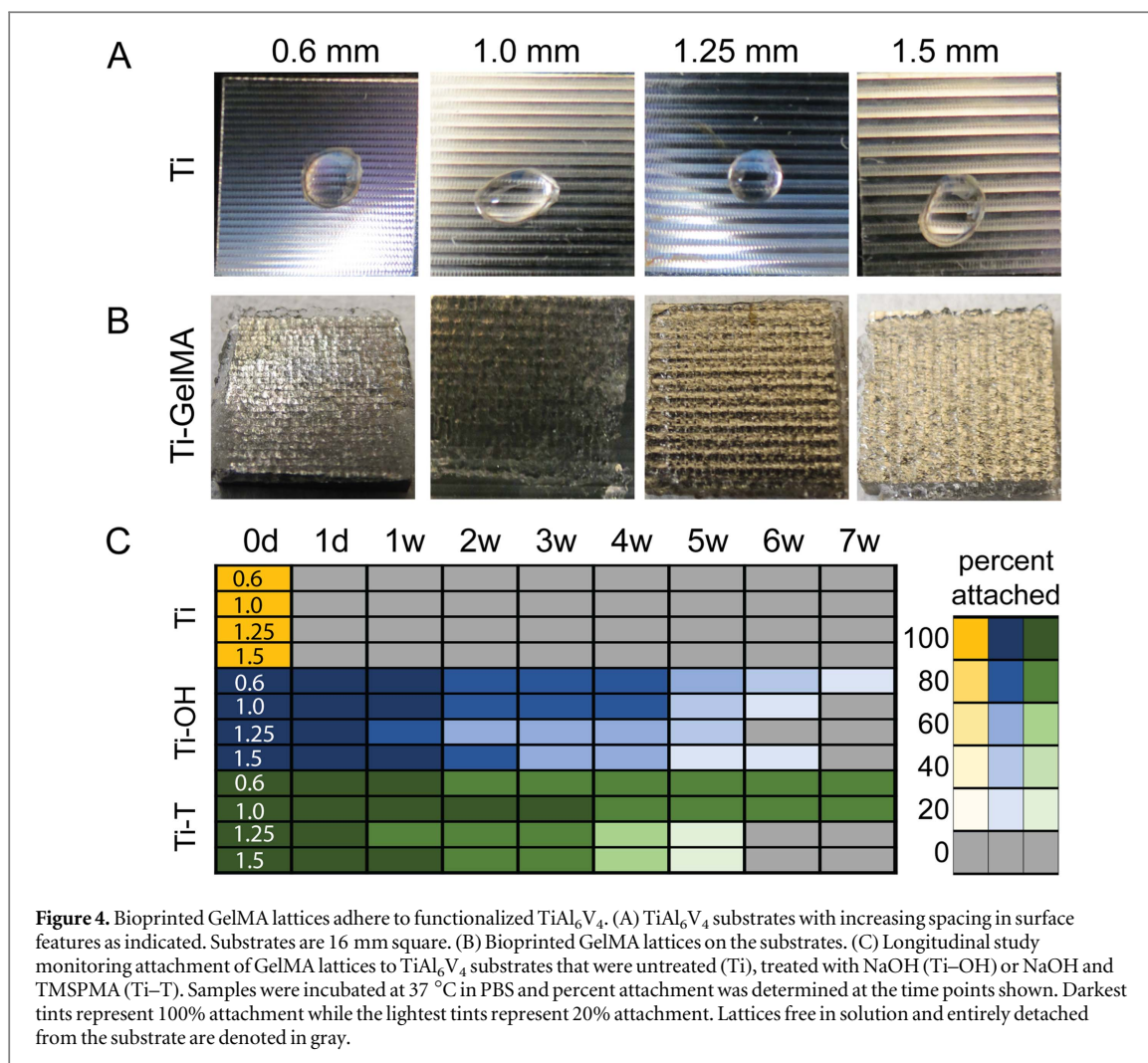
femoral head is surgically removed and the exposed femoral marrow is broached and reamed to create room for the implant. While the GelMA hydrogels were durable in solution, we tested the adherence of GelMA to titanium alloy in an animal marrow implantation model. We functionalized TiAl₆V₄ implants with a NaOH/TMSPMA treatment as before and grafted a GelMA film to the surface (figure 5(A)). We then breached and reamed porcine rib marrow with piezoelectric tools that matched the dimensions of the implant to allow a tight press fit into the marrow. After the implant head was flush with the cut bone surface, we extracted the implant. While portions of the GelMA film remained grafted after removal, substantial portions of the soft hydrogel were sheared during implantation, highlighting the need for a protective groove system within the titanium implant itself.

To demonstrate feasibility of this approach, we fabricated titanium alloy rods with radial grooves and functionalized the implants as before (figure 5(B)). The scale of the implant groove features was designed to match the approximate groove dimensions of the final implant however the central post is much narrower to accommodate the width of the marrow model. GelMA lattices were hand printed radially into the grooves and UV cured prior to implantation. Sample mass measured before and after implantation demonstrated that only 6% (16 mg) of the hydrogel was lost during implantation. These straightforward marrow implantation models provide a rapid mechanism for iteratively testing grafting chemistries and implant geometries prior to more extensive live animal models.

Discussion

Improving osseointegration of titanium implants to prevent aseptic loosening and ultimate surgical revisions has primarily focused on altering the surface of the titanium to trigger migrating osteoblasts to deposit new mineral. These implant surfaces are grit blasted, acid etched, plasma sprayed, or otherwise treated in an effort to increase surface roughness, which has been demonstrated to trigger differentiation of osteoblasts [45]. However, the hierarchy of the diverse array of mechanical and biological factors that contribute to a fully mature osteoblast lineage commitment has remained unclear.

Here, MG63 osteoblasts were seeded onto both glass coverslips and a GelMA hydrogel film with a viscoelastic storage modulus on the order of 1 kPa. Phalloidin staining of F-actin demonstrated that the cells formed significant levels of stress fibers when grown on hydrogel films as compared to glass. Stress fibers are correlated with lower levels of differentiation in response to a variety of environmental cues including surface roughness [31, 46], material elasticity [35, 47–



49], cellular compression [50], and BMP2 [51]. The importance of the actin cytoskeleton in downstream differentiation is highlighted by the fact that cytochalasin D, which disrupts actin filament formation, increases osteoblast differentiation at levels comparable to osteogenic media [52].

In our studies, calcium mineral deposition, which is the clearest indicator of osteoblast differentiation, was absent in cells grown on GelMA hydrogel films. However, when the same GelMA hydrogel was bioprinted into a three-dimensional porous scaffold, both MG63 osteoblasts and, importantly, primary NHOst cells deposited new calcium mineral. This suggests that the environmental cues provided by the three-dimensional lattice can override the mechanical cue of material elasticity. This view is supported by work done with porous titanium in which cells growing on non-porous titanium controls exhibit lower levels of differentiation markers [37] and low levels of osseointegration in a minipig model [53] when compared to similarly stiff porous titanium implants. We note that in these cases, porosity cannot be dissected from surface roughness as the manufacturing methods used to generate the porous implants were also necessarily rough ($R_a > 20 \mu\text{m}$, where measured). This is true as

well for the porous GelMA scaffold here as the extrusion process may have micropitted the material prior to UV curing. These scaffolds can be directly grafted to the titanium implant provided that the hydrogel is protected within grooves. Such radial grooves imbedded with GelMA lattices could promote bone ingrowth and facilitate the formation of an effective dovetail joint along the length of the implant [54].

Adhesion to rough titanium surfaces is primarily mediated through $\alpha_5\beta_1$ integrin which is also responsible for binding to fibronectin, osteopontin, and other extracellular protein components of bone [29, 55, 56]. However, adhesion to collagen and therefore gelatin-based derivatives is mediated through four separate integrins ($\alpha_1\beta_1$, $\alpha_2\beta_1$, $\alpha_{10}\beta_1$, $\alpha_{11}\beta_1$) highlighting a small part of the complexity of the systems osteoblasts use to sense their environments. How osteoblasts integrate these diverse signals into a committed decision to differentiate is an active area of research and determining hierarchy will be critical. This information can be incorporated into materials and coatings focused on differentiation cues that can be ignored and those that cannot. Our work suggests that the biological cues provided by the gelatin were less important than the mechanical cues of the three-

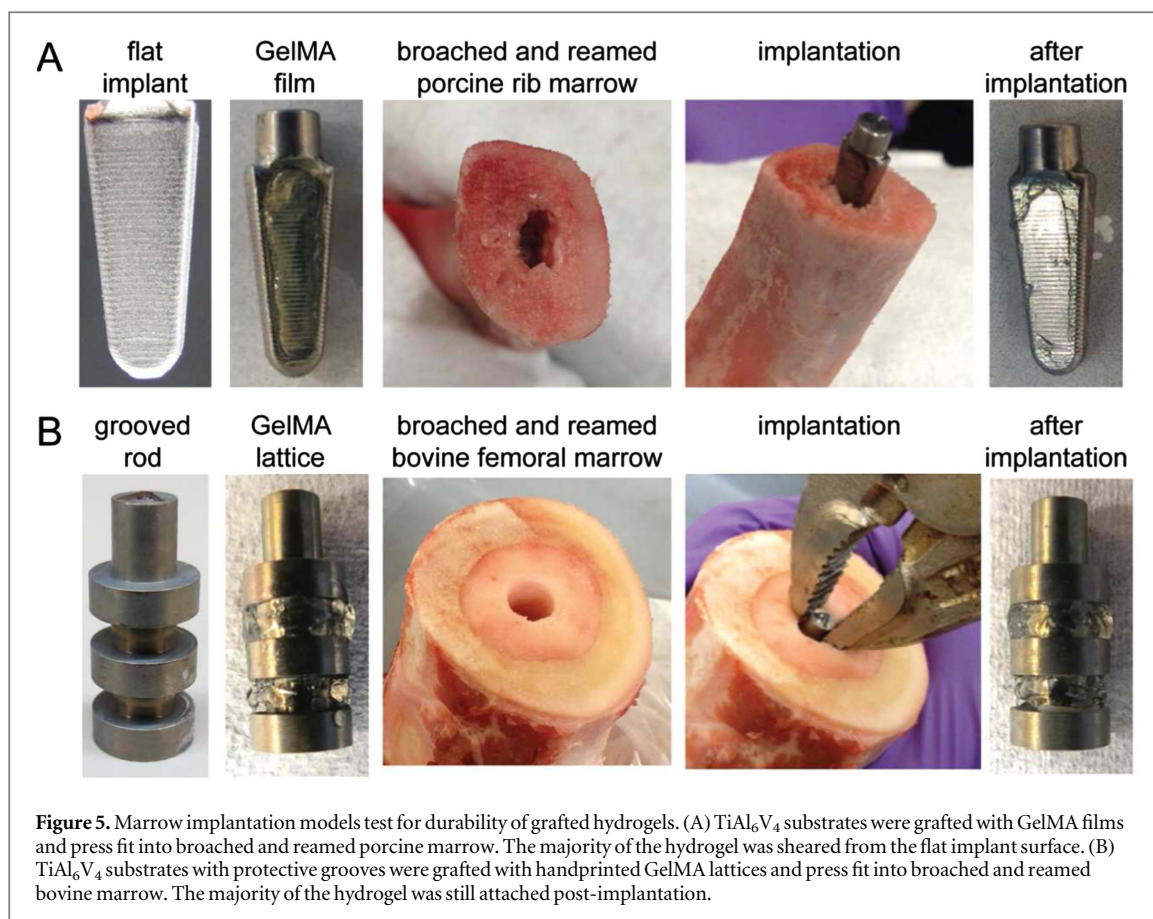


Figure 5. Marrow implantation models test for durability of grafted hydrogels. (A) TiAl_6V_4 substrates were grafted with GelMA films and press fit into broached and reamed porcine marrow. The majority of the hydrogel was sheared from the flat implant surface. (B) TiAl_6V_4 substrates with protective grooves were grafted with handprinted GelMA lattices and press fit into broached and reamed bovine marrow. The majority of the hydrogel was still attached post-implantation.

dimensional lattice. As mechanical cues such as porosity and roughness can be provided for by titanium, the advantage of the hydrogel may be in delivering factors over a 2–3 week period. Such delivery could include antibiotics to contravene infection at the time of surgery, hydroxyapatite nanoparticles with reduced risk of later debridement of the joint, and osteoinductive factors such as BMP-2 as the hydrogel is digested by cellular collagenases.

Acknowledgments

We would like to thank Egor Sedov for his contribution to this work. This work was funded by Fraunhofer USA and Fraunhofer Gesellschaft Theranostische Implantate.

References

- [1] Chatakun P, Nunez-Toldra R, Diaz Lopez E J, Gil-Recio C, Martinez-Sarra E, Hernandez-Alfaro F, Ferrer-Padro E, Giner-Tarrida L and Atari M 2014 The effect of five proteins on stem cells used for osteoblast differentiation and proliferation: a current review of the literature *Cell. Mol. Life Sci.* **71** 113–42
- [2] Zhang B G, Myers D E, Wallace G G, Brandt M and Choong P F 2014 Bioactive coatings for orthopaedic implants—recent trends in development of implant coatings *Int. J. Mol. Sci.* **15** 11878–921
- [3] Hori N, Iwasa F, Ueno T, Takeuchi K, Tsukimura N, Yamada M, Hattori M, Yamamoto A and Ogawa T 2010 Selective cell affinity of biomimetic micro–nano–hybrid structured TiO_2 overcomes the biological dilemma of osteoblasts *Dental Mater.* **26** 275–87
- [4] Schwartz Z, Lohmann C H, Oefinger J, Bonewald L F, Dean D D and Boyan B D 1999 Implant surface characteristics modulate differentiation behavior of cells in the osteoblastic lineage *Adv. Dental Res.* **13** 38–48
- [5] Roohani-Esfahani S I, Nouri-Khorasani S, Lu Z, Appleyard R and Zreiqat H 2010 The influence hydroxyapatite nanoparticle shape and size on the properties of biphasic calcium phosphate scaffolds coated with hydroxyapatite-PCL composites *Biomaterials* **31** 5498–509
- [6] Cavalcanti-Adam E A, Shapiro I M, Composto R J, Macarak E J and Adams C S 2002 RGD peptides immobilized on a mechanically deformable surface promote osteoblast differentiation *J. Bone Miner. Res.* **17** 2130–40
- [7] Ferris D M, Moodie G D, Dimond P M, Gioranni C W, Ehrlich M G and Valentini R F 1999 RGD-coated titanium implants stimulate increased bone formation *in vivo* *Biomaterials* **20** 2323–31
- [8] Gruber R M, Krohn S, Mauth C, Dard M, Molenberg A, Lange K, Perske C and Schliephake H 2014 Mandibular reconstruction using a calcium phosphate/polyethylene glycol hydrogel carrier with BMP-2 *J. Clin. Periodontol.* **41** 820–6
- [9] Betz M W, Caccamese J F, Coletti D P, Sauk J J and Fisher J P 2009 Tissue response and orbital floor regeneration using cyclic acetal hydrogels *J. Biomed. Mater. Res. A* **90** 819–29
- [10] Igarashi M, Kamiya N, Hasegawa M, Kasuya T, Takahashi T and Takagi M 2004 Inductive effects of dexamethasone on the gene expression of Cbfa1, Osterix and bone matrix proteins during differentiation of cultured primary rat osteoblasts *J. Mol. Histol.* **35** 3–10
- [11] Yang H W, Lin M H, Xu Y Z, Shang G W, Wang R R and Chen K 2015 Osteogenesis of bone marrow mesenchymal stem cells on strontium-substituted nano-hydroxyapatite coated roughened titanium surfaces *Int. J. Clin. Exp. Med.* **8** 257–64
- [12] Lincks J, Boyan B D, Blanchard C R, Lohmann C H, Liu Y, Cochran D L, Dean D D and Schwartz Z 1998 Response of

- MG63 osteoblast-like cells to titanium and titanium alloy is dependent on surface roughness and composition *Biomaterials* **19** 2219–32
- [13] Graves D T and Cochran D L 1994 Periodontal regeneration with polypeptide growth factors *Curr. Opin. Periodontol.* 178–86
- [14] Engler A J, Sen S, Sweeney H L and Discher D E 2006 Matrix elasticity directs stem cell lineage specification *Cell* **126** 677–89
- [15] Wieding J, Wolf A and Bader R 2014 Numerical optimization of open-porous bone scaffold structures to match the elastic properties of human cortical bone *J. Mech. Behav. Biomed. Mater.* **37** 56–68
- [16] Zhang L L, Hanagata N, Maeda M, Minowa T, Ikoma T, Fan H and Zhang X D 2009 Porous hydroxyapatite and biphasic calcium phosphate ceramics promote ectopic osteoblast differentiation from mesenchymal stem cells *Sci. Technol. Adv. Mat.* **10** 025003
- [17] Black C R, Goriainov V, Gibbs D, Kanczler J, Tare R S and Oreffo R O 2015 Bone tissue engineering *Curr. Mol. Biol. Rep.* **1** 132–40
- [18] Chen F M, Zhao Y M, Sun H H, Jin T, Wang Q T, Zhou W, Wu Z F and Jin Y 2007 Novel glycidyl methacrylated dextran (Dex-GMA)/gelatin hydrogel scaffolds containing microspheres loaded with bone morphogenetic proteins: formulation and characteristics *J. Control. Rel.* **118** 65–77
- [19] Williams J M, Adewunmi A, Schek R M, Flanagan C L, Krebsbach P H, Feinberg S E, Hollister S J and Das S 2005 Bone tissue engineering using polycaprolactone scaffolds fabricated via selective laser sintering *Biomaterials* **26** 4817–27
- [20] Yue K, Trujillo-de Santiago G, Alvarez M M, Tamayol A, Annabi N and Khademhosseini A 2015 Synthesis, properties, and biomedical applications of gelatin methacryloyl (GelMA) hydrogels *Biomaterials* **73** 254–71
- [21] Klotz B J, Gawlitta D, Rosenberg A J, Malda J and Melchels F P 2016 Gelatin–methacryloyl hydrogels: towards biofabrication-based tissue repair *Trends Biotechnol.* **34** 394–407
- [22] Tan G X, Zhou L, Ning C Y, Tan Y, Ni G X, Liao J W, Yu P and Chen X F 2013 Biomimetically mineralized composite coatings on titanium functionalized with gelatin methacrylate hydrogels *Appl. Surf. Sci.* **279** 293–9
- [23] Campbell J M I, Wirz H, Sharon A and Sauer-Budge A F 2015 Multimaterial and multiscale three-dimensional bioprinter *ASME J. Nanotechnol. Eng. Med.* **6** 021005
- [24] Xiao W Q, He J K, Nichol J W, Wang L Y, Hutson C B, Wang B, Du Y A, Fan H S and Khademhosseini A 2011 Synthesis and characterization of photocrosslinkable gelatin and silk fibroin interpenetrating polymer network hydrogels *Acta Biomater.* **7** 2384–93
- [25] Mattioli-Belmonte M, Cometa S, Ferretti C, Iatta R, Trapani A, Ceci E, Falconi M and De Giglio E 2014 Characterization and cytocompatibility of an antibiotic/chitosan/cyclodextrins nanocoating on titanium implants *Carbohydr. Polym.* **110** 173–82
- [26] Ulrich S D et al 2008 Total hip arthroplasties: what are the reasons for revision? *Int. Orthopaedics* **32** 597–604
- [27] de Vasconcellos L M, Oliveira F N, Leite D de O, de Vasconcellos L G, do Prado R F, Ramos C J, Graca M L, Cairo C A and Carvalho Y R 2012 Novel production method of porous surface Ti samples for biomedical application *J. Mater. Sci. Mater. Med.* **23** 357–64
- [28] Van Den Bulcke A I, Bogdanov B, De Rooze N, Schacht E H, Cornelissen M and Berghmans H 2000 Structural and rheological properties of methacrylamide modified gelatin hydrogels *Biomacromolecules* **1** 31–8
- [29] Wei Q, Pohl T L M, Seckinger A, Spatz J P and Cavalcanti-Adam E A 2015 Regulation of integrin and growth factor signaling in biomaterials for osteodifferentiation *Beilstein J. Org. Chem.* **11** 773–83
- [30] Han F X, Zhu C H, Guo Q P, Yang H L and Li B 2016 Cellular modulation by the elasticity of biomaterials *J. Mater. Chem. B* **4** 9–26
- [31] Bergemann C, Duske K, Nebe J B, Schone A, Bulnheim U, Seitz H and Fischer J 2015 Microstructured zirconia surfaces modulate osteogenic marker genes in human primary osteoblasts *J. Mater. Sci.* **26** 5350
- [32] Bachle M and Kohal R J 2004 A systematic review of the influence of different titanium surfaces on proliferation, differentiation and protein synthesis of osteoblast-like MG63 cells *Clin. Oral Impl. Res.* **15** 683–92
- [33] Czekanska E M, Stoddart M J, Richards R G and Hayes J S 2012 In search of an osteoblast cell model for *in vitro* research *Eur. Cells Mater.* **24** 1–17
- [34] Czekanska E M, Stoddart M J, Ralphs J R, Richards R G and Hayes J S 2014 A phenotypic comparison of osteoblast cell lines versus human primary osteoblasts for biomaterials testing *J. Biomed. Mater. Res. A* **102** 2636–43
- [35] Tsai S W, Liou H M, Lin C J, Kuo K L, Hung S, Weng R C and Hsu F Y 2012 MG63 osteoblast-like cells exhibit different behavior when grown on electrospun collagen matrix versus electrospun gelatin matrix *PLoS One* **7** e31200
- [36] Matschegewski C, Staehle S, Birkholz H, Lange R, Beck U, Engel K and Nebe J B 2012 Automatic actin filament quantification of osteoblasts and their morphometric analysis on microtextured silicon–titanium arrays *Materials* **5** 1176–95
- [37] St-Pierre J P, Gauthier M, Lefebvre L P and Tabrizian M 2005 Three-dimensional growth of differentiating MC3T3-E1 pre-osteoblasts on porous titanium scaffolds *Biomaterials* **26** 7319–28
- [38] Bertassoni L E et al 2014 Direct-write bioprinting of cell-laden methacrylated gelatin hydrogels *Biofabrication* **6** 024105
- [39] Gauvin R, Chen Y C, Lee J W, Soman P, Zorlutuna P, Nichol J W, Bae H, Chen S C and Khademhosseini A 2012 Microfabrication of complex porous tissue engineering scaffolds using 3D projection stereolithography *Biomaterials* **33** 3824–34
- [40] Billiet T, Gevaert E, De Schryver T, Cornelissen M and Dubrue P 2014 The 3D printing of gelatin methacrylamide cell-laden tissue-engineered constructs with high cell viability *Biomaterials* **35** 49–62
- [41] Schuurman W, Levett P A, Pot M W, van Weeren P R, Dhert W J A, Huttmacher D W, Melchels F P W, Klein T J and Malda J 2013 Gelatin–methacrylamide hydrogels as potential biomaterials for fabrication of tissue-engineered cartilage constructs *Macromol. Biosci.* **13** 551–61
- [42] Choi J Y, Konno T, Matsuno R, Takai M and Ishihara K 2008 Surface immobilization of biocompatible phospholipid polymer multilayered hydrogel on titanium alloy *Colloid Surf. B* **67** 216–23
- [43] Navarro R, Perrino M P, Prucker O and Ruhe J 2013 Preparation of surface-attached polymer layers by thermal or photochemical activation of alpha-diazoester moieties *Langmuir* **29** 10932–9
- [44] Niinomi M 1998 Mechanical properties of biomedical titanium alloys *Mater. Sci. Eng. A* **243** 231–6
- [45] Shibata Y and Tanimoto Y 2015 A review of improved fixation methods for dental implants: I. Surface optimization for rapid osseointegration *J. Prosthodontic Res.* **59** 20–33
- [46] Okumura A, Goto M, Goto T, Yoshinari M, Masuko S, Katsuki T and Tanaka T 2001 Substrate affects the initial attachment and subsequent behavior of human osteoblastic cells (Saos-2) *Biomaterials* **22** 2263–71
- [47] Trappmann B et al 2012 Extracellular-matrix tethering regulates stem-cell fate *Nat. Mater.* **11** 642–9
- [48] Discher D E, Mooney D J and Zandstra P W 2009 Growth factors, matrices, and forces combine and control stem cells *Science* **324** 1673–7
- [49] Thiele J, Ma Y J, Brueckers S M C, Ma S H and Huck W T S 2014 25th anniversary article: designer hydrogels for cell cultures: a materials selection guide *Adv. Mater.* **26** 125–48
- [50] Li J, Chen G P, Zheng L L, Luo S J and Zhao Z H 2007 Osteoblast cytoskeletal modulation in response to compressive stress at physiological levels *Mol. Cell. Biochem.* **304** 45–52
- [51] Gamell C, Osses N, Bartrons R, Rueckle T, Camps M, Rosa J L and Ventura F 2008 BMP2 induction of actin cytoskeleton reorganization and cell migration requires PI3-kinase and Cdc42 activity *J. Cell Sci.* **121** 3960–70

- [52] Rodriguez J P, Gonzalez M, Rios S and Cambiazo V 2004 Cytoskeletal organization of human mesenchymal stem cells (MSC) changes during their osteogenic differentiation *J. Cell. Biochem.* **93** 721–31
- [53] Schwarz M L R, Kowarsch M, Rose S, Becker K, Lenz T and Jani L 2009 Effect of surface roughness, porosity, and a resorbable calcium phosphate coating on osseointegration of titanium in a minipig model *J. Biomed. Mater. Res. A* **89A** 667–78
- [54] Hayashi K, Mashima T and Uenoyama K 1999 The effect of hydroxyapatite coating on bony ingrowth into grooved titanium implants *Biomaterials* **20** 111–9
- [55] Luthen F, Lange R, Becker P, Rychly J, Beck U and Nebe J G B 2005 The influence of surface roughness of titanium on beta 1- and beta 3-integrin adhesion and the organization of fibronectin in human osteoblastic cells *Biomaterials* **26** 2423–40
- [56] Wang L P, Zhao G, Olivares-Navarrete R, Bell B F, Wieland M, Cochran D L, Schwartz Z and Boyan B D 2006 Integrin beta(1) silencing in osteoblasts alters substrate-dependent responses to 1, 25-dihydroxy vitamin D-3 *Biomaterials* **27** 3716–25